

Longitudinal volume viscosity of 1,2 syndiotactic polybutadiene

J. V. Aleman

Instituto de Plasticos y Caucho, Juan de la Cierva 3, Madrid 28006, Spain

(Received 7 October 1987; revised 22 December 1987; accepted 15 March 1988)

The volume flow of 1,2 syndiotactic polybutadiene (1,2 s-PB) ($\bar{M}_n = 90\,500$, $T_m = 373\text{ K}$ and $T_g = 262\text{ K}$) has been measured. The elastic modulus of the longitudinal wave, the longitudinal volume viscosity, the initial longitudinal volume viscosity and retardation times are described at compression rates of $\sim 1.0 \times 10^{-5}$ – $200.0 \times 10^{-5}\text{ s}^{-1}$, and at temperatures of 403–423 K and pressures up to 150 MPa. Longitudinal volume viscosity decreases with increasing compression rate, and with decreasing volume deformation, the behaviour being in all cases typical non-equilibrium behaviour. Longitudinal volume viscosity increases with increasing temperature, the volume flow activation energy being $\sim 56.3\text{ kJ mol}^{-1}$.

(Keywords: polymer; volume viscosity; melt compressibility)

INTRODUCTION

A study of the effect of molecular structure on the compression behaviour of polymers began recently. It led to the conclusion that polymer rheological behaviour in compression is governed mainly by two molecular parameters: chain conformation (helicoïdal, planar) and chain rigidity (from $\sim 500\text{ J g}^{-1}$ to 200 J g^{-1}).

The polymers tested to date for this purpose are the following:

1. helicoïdal polymers with one rigid side-group, such as polystyrene¹; two flexible side-groups, such as poly(methyl methacrylate)²; one flexible side-group, such as isotactic polypropylene³; and no side-group, such as poly(ethylene oxide)⁴; and

2. linear planar polymers (zig-zag conformation), (a) with aromatic rings and no side-groups, such as poly(butylene terephthalate)⁵, and two side-groups, like the epoxide prepolymers⁶; (b) with aliphatic chains with one side-group, such as poly(vinyl chloride)⁷.

(See Table 1, in which the chain rigidity is considered to be the Gibbs free energy at 450 K ($-\Delta F^{450\text{K}}$) (ref. 2) computed from specific heat *versus* temperature curves such as those of Figure 1 for 1,2 s-PB.)

Polybutadiene differs from these polymers in that it contains double bonds, which allow it to exhibit different isomeric forms and conformations^{8,9}: 1-4 *cis* (skewed

Table 1 Molecular characteristics of polymers

Polymer	Formula	Conformation	Rigidity (J g^{-1})	Tacticity
PMMA	$\begin{array}{c} \text{CH}_3 \\ \\ \text{---CH}_2\text{---C---} \\ \\ \text{COOCH}_3 \end{array}$	Helicoïdal	561	
1,2 s-PB	$\begin{array}{c} \text{---CH}_2\text{---CH---} \\ \\ \text{C}_2\text{H}_5 \end{array}$	Planar	547	Syndiotactic
i-PP	$\begin{array}{c} \text{---CH}_2\text{---CH---} \\ \\ \text{CH}_3 \end{array}$	Helicoïdal	543	Isotactic
PS	$\begin{array}{c} \text{---CH}_2\text{---CH---} \\ \\ \text{C}_6\text{H}_5 \end{array}$	Helicoïdal	490	
PEO	$\text{---CH}_2\text{---CH}_2\text{---O---}$	Helix/planar	181	
EP	$\text{---R'---O---}\left[\text{R---O---CH}_2\text{---}\overset{\text{OH}}{\underset{ }{\text{CH}}}\text{---CH}_2\text{---O}\right]_n\text{---R---R'}$	Planar	406	$\left\{ \begin{array}{l} \text{R} = \text{---C}_6\text{H}_4\text{---C(CH}_3)_2\text{---C}_6\text{H}_4\text{---} \\ \text{R}' = \begin{array}{c} \text{O} \\ \diagup \quad \diagdown \\ \text{CH}_2\text{---CH---} \end{array} \end{array} \right.$
PBT	$\text{---O---OC---C}_6\text{H}_4\text{---CO---O---(CH}_2)_4\text{---}$	Planar	458	
PVC	$\begin{array}{c} \text{---CH}_2\text{---CH---} \\ \\ \text{Cl} \end{array}$	Planar	503	

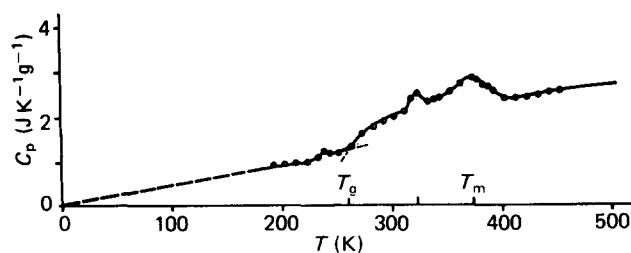


Figure 1 1,2 s-PB specific heat (C_p) as a function of temperature

helix), 1-4 *trans* (skewed helix), 1-2 isotactic (helix) and 1-2 syndiotactic (planar slightly deflected).

Since their compression behaviour has received scarce (mostly as cross-linked rubbers^{10,11}) or no attention, and their volume viscosity* has not been described to date, it is our purpose to measure these characteristics of the isomers which are available in sufficient amounts, beginning with the 1,2 syndiotactic polybutadiene (1,2 s-PB), which is the subject of this Paper.

This Paper will also give a better knowledge of how the rheological behaviour of polymers varies with their stereochemical conformation, by comparing 1,2 s-PB with isotactic polypropylene, i-PP³, which is also rigid with short side-groups and helicoidal.

EXPERIMENTAL

Material

The 1,2 syndiotactic polybutadiene used was JSR RB 830 from the Japan Synthetic Rubber Company, with 93% 1,2 units, 15–29% crystallinity and melt index 3.0 g/10 min¹².

Its number-average molecular weight ($\bar{M}_n = 90\,500$) was measured at 298 K from a 0.5% toluene solution, with the aid of the equation¹³:

$$[\eta] = 11.0 \times 10^{-4} \bar{M}_n^{0.62} \quad (2)$$

Its specific heat (C_p) was measured in a Mettler DSC 30 TC 10 TA processor, at a heating rate of 10 K min⁻¹. The

* Longitudinal (unidirectional or axial) volume viscosity (η_L) is the change in pressure which takes place, per unit compression rate, when the compression is in a direction parallel to the applied stress (as in a cylinder). It is related to the shear viscosity (η_G) and the volume (tridimensional or isotropic) viscosity (η_K) by the equation^{21,6}:

$$\eta_L = \eta_K + \frac{4}{3} \eta_G \quad (1)$$

η_K is sometimes called bulk viscosity and dilatational viscosity, and is defined as²²:

$$\eta_K = \frac{\Delta P}{\alpha \frac{dT}{dt} + \beta \frac{dP}{dt} - \frac{1}{V} \frac{dV}{dt}} \quad (1a)$$

where α is the thermal expansion coefficient

$$\alpha = \left(\frac{1}{V} \frac{dV}{dT} \right)_P$$

and β is the coefficient of compressibility

$$\beta = \left(\frac{1}{V} \frac{dV}{dP} \right)_T$$

For isothermal and isobaric systems equation (1a) reduces to:

$$\eta_K = \frac{-\Delta P}{\frac{1}{V} \frac{dV}{dt}} = \frac{-\Delta P}{\text{div } v} \quad (1b)$$

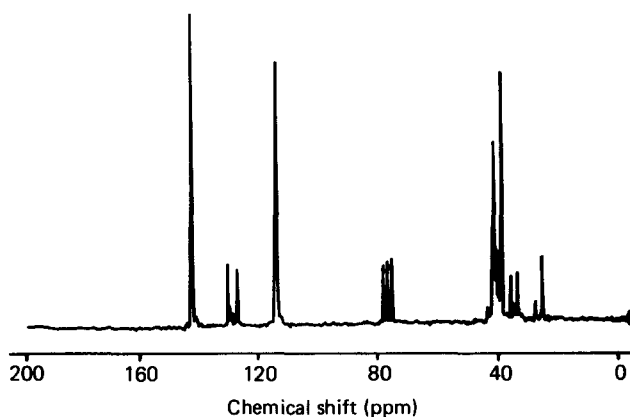


Figure 2 1,2 s-PB ¹³C n.m.r. spectra in CDCl₃

results are shown in Figure 1, according to which the 1,2 s-PB glass transition temperature is $T_g = 262$ K, and the melting temperature is $T_m = 373$ K. Also evident are the melting regions of 1,4 *cis* PB ($T_m = 238$ K)¹⁴, and 1,4 *trans* PB ($T_m = 323$ K)¹⁴. These different components were also identified with ¹³C nuclear magnetic resonance (n.m.r.) spectra in CDCl₃ (Figure 2)^{15,16}.

Method

All compression measurements were made in an Instron capillary rheometer attached to an Instron tensile tester model TT-CM, with a steel plug instead of the capillary, as described elsewhere⁶.

Into the rheometer barrel (area $A = 0.709$ cm²) were placed 4.5 g of 1,2 s-PB pellets, which were preheated to the run temperatures of 403–423 K, under a vacuum of about 130 Pa, for the adsorbed water to evolve. The equilibrium in force (F) and temperature (T) was attained under a load of 10 kg (1.38 MPa).

The dial reading provided the initial length l_i from which the polymer initial length l_0 was computed as:

$$l_0 = l_i + l_s - l_r \quad (3)$$

where l_s is the plunger travel security length and l_r the length of the Rulon plug. Thus it is possible to know the initial volume of polymer ($V_{T,\text{exp}}$).

The machine cross-head was lowered at selected rates (v_c), usually 0.035, 0.085, 0.17, 0.35 and 0.85×10^{-2} cm s⁻¹. The length of the polymer at any time (l_t) could be calculated for a given v_c :

$$l_t = l_i + l_s - (\Delta l_t)_P - (l_r)_P + (\Delta l_{\text{app}})_P - (\Delta l_{\text{polym}})_P \quad (4)$$

where:

$(\Delta l_t)_P$ = change in length
= machine cross-head speed \times time
= $v_c t$;

$(\Delta l_{\text{app}})_P$ = compliance (background response of the apparatus) measured as change in pressure *versus* change in length at 412 K with no polymer in the barrel, Figure 3;

$(\Delta l_{\text{polym}})_P$ = pressure absorbed by the polymer (some 12.0%)^{*} (Figure 3);

$l_{r,t}$ = length of the Rulon plug at time t .

* The weight of a cylinder is:

$$dw = dV \rho = \pi R^2 dl \quad (4a)$$

from which:

$$\frac{dP}{dl} = \frac{1}{A} \frac{dw}{dl} = \frac{\pi R^2 \rho}{A} \quad (4b)$$

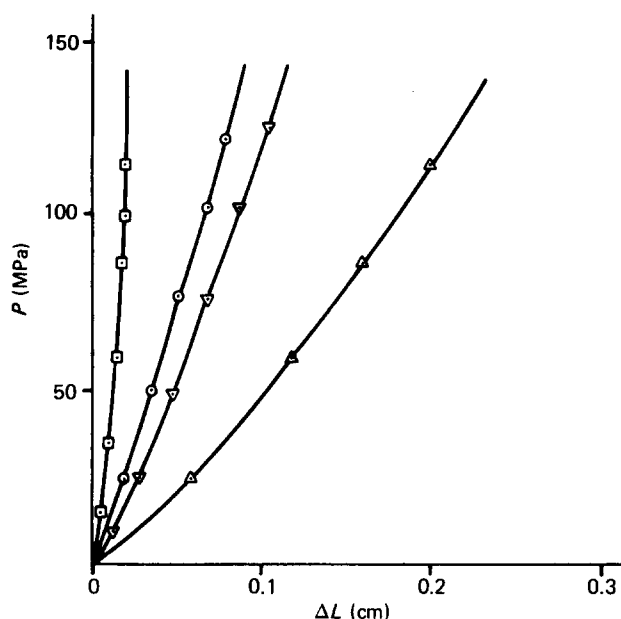


Figure 3 Background response, at 412 K and cross-head speed $0.034 \times 10^{-2} \text{ cm s}^{-1}$, of: \square , the Rulon plug; \odot , the apparatus; \triangle , the reference Rulon cylinder; and ∇ , the Rulon plug, apparatus and polymer

The changes in length Δl_r (Figure 3) are computed from the change in length at 412 K of a Rulon cylinder 3.2 cm high and 0.95 cm in diameter, $\Delta l_{R,t}$ (Figure 3)¹⁷:

$$(\Delta l_{r,t})_P = \frac{(V_r)_{0.1 \text{ MPa}} (\Delta l_{R,t})_P}{(V_R)_{0.1 \text{ MPa}}} \quad (5)$$

where $(V_r)_{0.1 \text{ MPa}}$ = volume of Rulon plug, and $(V_R)_{0.1 \text{ MPa}}$ = volume of Rulon cylinder, both at atmospheric pressure (0.1 MPa):

$$(\Delta l_{r,t})_P = (\Delta l_t)_P + (\Delta l_{app})_P \quad (6)$$

From this:

$$(l_{r,t})_P = l_r - (\Delta l_{r,t})_P \quad (7)$$

With l_r (equation (4)) the volume of the polymer at any time (V_t) may be computed. Combining it with $V_{T,exp}$ provides the change in volume of the sample (ΔV) with an uncertainty of about 2%:

$$\Delta V = V_t - V_{T,exp} \quad (8)$$

Force was registered on the Instron graph-paper, which moved at known rates of $5.0\text{--}50.0 \times 10^{-2} \text{ cm s}^{-1}$ according to the cross-head speed being used. It was also a measure of the time of the experiment (t). When the maximum force of about 1200 kg was reached, decompression was started at the same rate as in the compression step.

RESULTS AND DISCUSSION

Volume changes (ΔV) of the molten samples were measured in relation to: temperature (T); pressure (P) as force (F) per unit area (A):

$$P = F/A \quad (9)$$

volume deformation ($k\%$) defined as the change in volume (ΔV) per unit volume at the temperature of the

experiment ($V_{T,exp}$):

$$k\% = \frac{\Delta V}{V_{T,exp}} \times 100 \quad (10)$$

and compression rate (\dot{k}) equal to the change in volume deformation ($k\%$) per unit time (t):

$$\dot{k} = \frac{dk}{dt} = \frac{1}{V_{T,exp}} \frac{\Delta V}{\Delta t} \quad (11)$$

The effect of these process variables on the rheological behaviour of 1,2 s-PB in compression may be described as follows.

Longitudinal volume viscosity (η_L)

Pressure changes $P(k)$ as a function of volume deformation ($k\%$) were measured at 403, 408, 412 and 423 K. Figure 4 (in which the 10 kg weight used during the pre-heating step was taken into account by shifting the lines to the right by 0.25%) shows a representative example, at 423 K.

With the $P(k)$ data thus obtained, the rheological parameters of the polymer were computed using the analytical procedure described elsewhere⁶.

The behaviour of the polymer is assumed to be represented by the Voigt-Kelvin element (spring and dashpot in parallel) of total stress (σ):

$$\sigma = \sigma_{visc} + \sigma_{elast} = -P \quad (12)$$

To eliminate the elastic component, an extrapolation to zero compression rate ($\dot{k}=0$) was carried out. Figure 5 shows a representative example, at 403 K.

Using this, the elastic modulus in longitudinal compression (L) was determined:

$$L = \frac{P(k)_{\dot{k}=0}}{k} \quad (13)$$

and its values are shown in Figure 6.

The longitudinal volume viscosity (η_L) was then computed as:

$$\eta_L = \frac{P(k) - L(k)k}{\dot{k}} = \frac{P(k) - P(k)_{\dot{k}=0}}{\dot{k}} \quad (14)$$

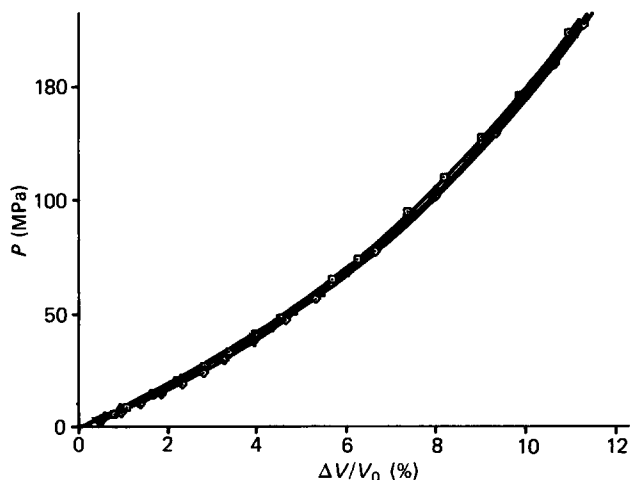


Figure 4 $P(k)$ data at $T=423 \text{ K}$ and different k ($\times 10^{-5} \text{ s}^{-1}$): \diamond , 4.37; \triangle , 21.8; \square , 109.5

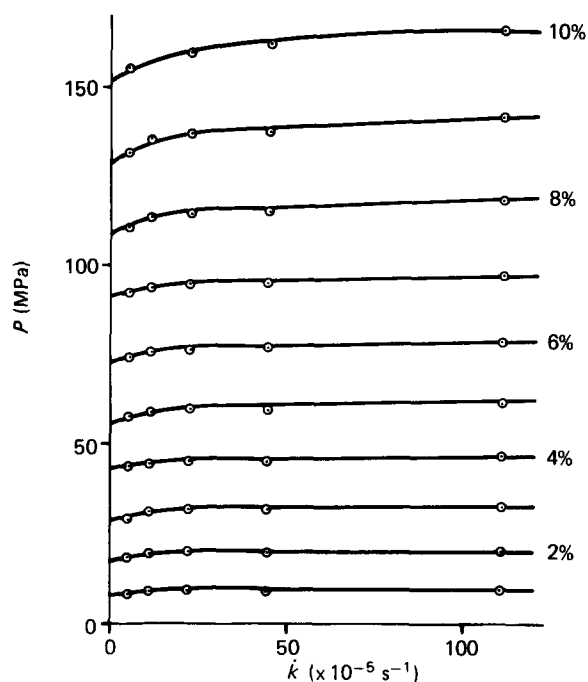


Figure 5 Extrapolation to zero compression rate (\dot{k}) at $T=403$ K

Effect of compression rate (\dot{k})

Temperatures of 403, 408, 412, 418 and 423 K, well above the 1,2 s-PB melting temperature ($T_m=373$ K), were used for the polymer to be fully in the melt region. Results are shown in Figure 7 at 403–423 K, as a function of compression rate (\dot{k}).

As the compression rate (\dot{k}) increases, in some cases the longitudinal volume viscosity (η_L) initially increases, and in other cases negative values of η_L are observed (compression zone) followed by an increase in η_L (elastic zone). Thereafter (at all temperatures and $k\%$), a steady decrease toward the limiting value $\eta_L=0$ at $\dot{k} \rightarrow \infty$ is observed.

A molecular interpretation of this behaviour is provided below.

Longitudinal volume viscosity (η_L) is related to volume viscosity (η_K , isotropic) and shear viscosity (η_G) by equation (1). Since the η_L of 1,2 s-PB have an average value of $\sim 0.1\text{--}0.2 \times 10^5$ MPa s, and the shear viscosity¹² of 1,2 s-PB, η_G , at 423 K is $\sim 2.0 \times 10^{-3}$ MPa s, the ratio $\eta_L/\eta_G=10^7$ shows that the longitudinal volume viscosity (η_L) is 10^7 times the shear viscosity (η_G). Equation (1) then reduces to $\eta_L \approx \eta_K$, i.e. the difference between the longitudinal volume viscosity (η_L) and the bulk viscosity (η_K) is negligible for 1,2 s-PB, as has also been shown to be the case for all other polymers tested¹⁻⁷.

With the longitudinal volume viscosities of Figure 7, the dashpot stress (σ_{visc}) was computed from the equation:

$$\sigma_{\text{visc}} = -\eta_L \dot{k} \quad (15)$$

Their values follow a similar pattern to that of Figure 7.

Effect of volume deformation ($k\%$)

Longitudinal volume viscosities (η_L) are plotted in Figure 8 at 403 and 423 K as a function of volume deformation ($k\%$). The 'initial' longitudinal volume viscosities (η_L^0 , Table 2) computed with the help of

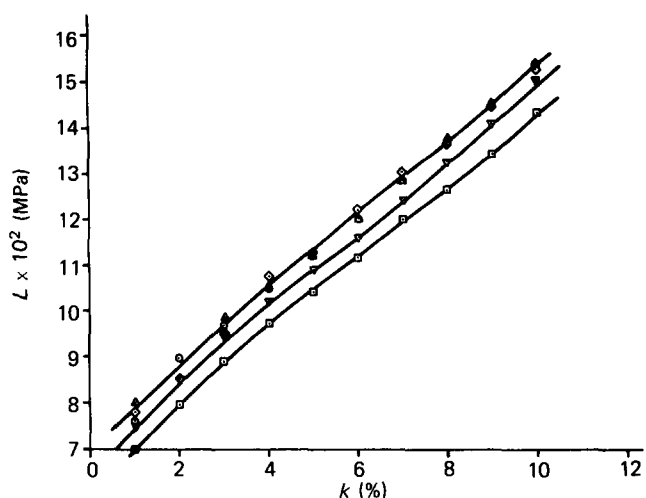


Figure 6 Elastic modulus (L) at: \diamond , 403 K; \circ , 408 K; \triangle , 412 K; ∇ , 418 K; and \square , 423 K

equation (15) and the initial* ($k=0, t=0$) dashpot stress $\sigma_{\text{visc}}^0 = 1.38$ MPa are also shown. η_L^0 is independent of the experimental temperature.

A sort of non-equilibrium behaviour is observed in all cases. Actually the polymer has not reached the equilibrium compression, as indicated by the progressively increasing non-linearity of the P versus k curves of Figure 5; at equilibrium they should be straight lines parallel to the abscissa axis; the 'waviness' of the curve is more pronounced the smaller the compression rate (\dot{k}). This has also been noted in other helicoidal polymers (PMMA)², and in planar polymers (EP⁶, PVC⁷, PBT⁵, etc.) though it was less pronounced in planar polymers, possibly due to their more compact structure.

The retardation time (τ) which characterizes the fundamental processes required for the readjustment of the structure or, what is the same, the time required to reach equilibrium, was computed with the equation:

$$\tau = \eta_L / L \quad (16)$$

and is shown in Figure 9 as a function of volume deformation ($k\%$) at 403 K and compression rates (\dot{k}) from 4.0×10^{-5} to $100.0 \times 10^{-5} \text{ s}^{-1}$. The curves follow a similar pattern to those of η_L versus $k\%$ (Figure 8), increasing with decreasing compression rate (\dot{k}).

No theoretical model is yet available for the nonlinear volume viscosity of polymers, although some scaling equations have been advanced¹.

The source of this peculiar behaviour is tentatively believed to be as follows:

The level of experimental temperature defines the initial volume of the sample ($V_{T,\text{exp}}$) (the temperature dependence of the unperturbed mean square end-to-end distance \bar{r}_0^2 reflects the difference in energy between the more or less extended conformations of the chain).

The pressure applied afterwards reduces the volume (pressure dependence of \bar{r}_0^2 reflects the difference in effective volume of the chains in various conformations). Consequently, η_L initially decreases, possibly due to an

* The weight of 10 kg used to reach the initial equilibrium in pressure and temperature is equivalent to a volume deformation of $\Delta V/V=0.20\%$. With it the 'initial' longitudinal volume viscosities η_L^0 of 1,2 s-PB were computed and are shown in Table 2.

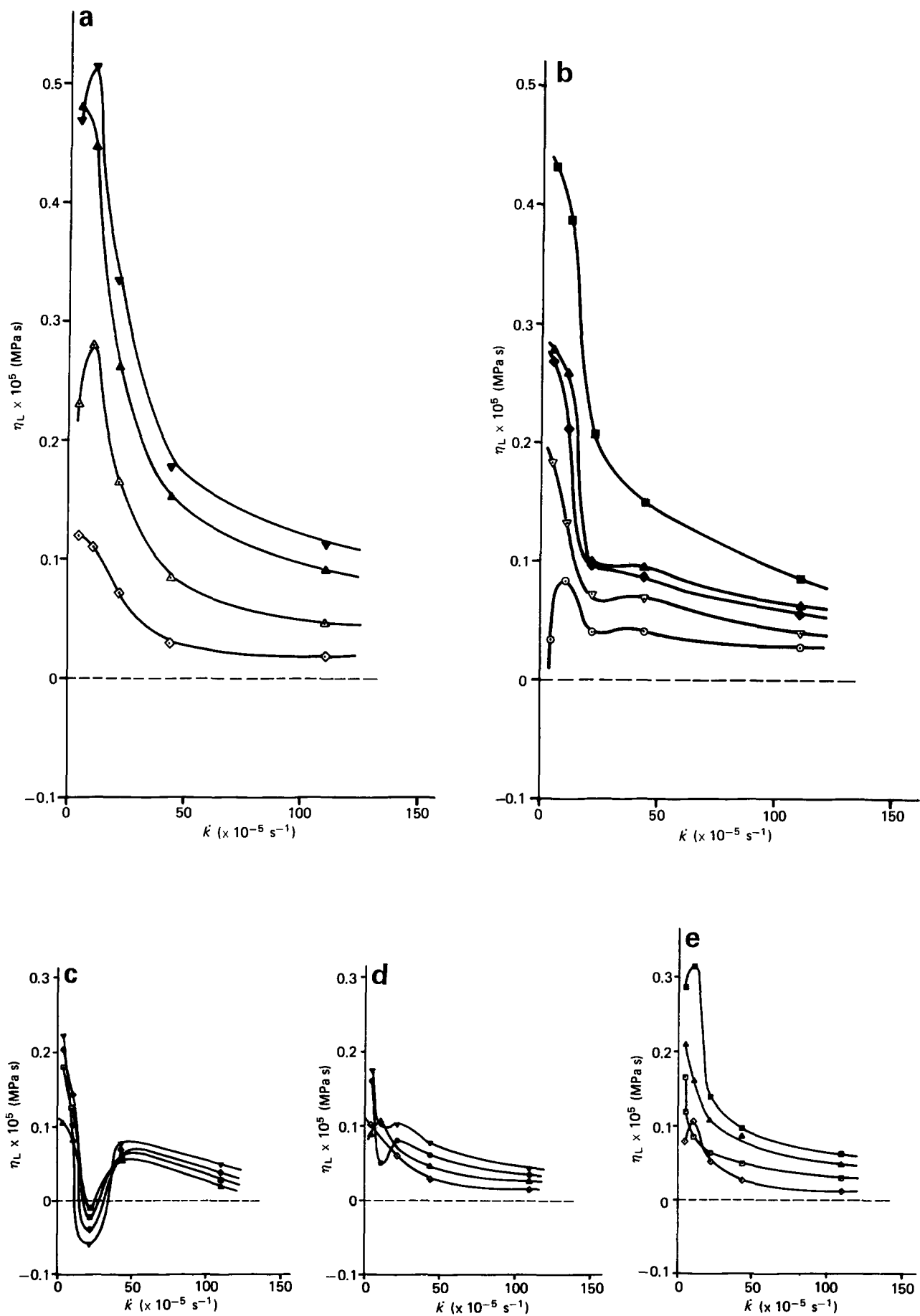


Figure 7 Longitudinal volume viscosity (η_L) at: (a) 403 K and different $k\%$: \diamond , 1; \triangle , 3; \blacktriangle , 8; and \blacktriangledown , 9; (b) 408 K and different $k\%$: \circ , 2; ∇ , 4; \blacklozenge , 6; \blacktriangle , 8; and \blacksquare , 10; (c) 412 K and different $k\%$: \triangle , 3; \square , 5; \blacklozenge , 6; and \blacktriangledown , 9; (d) 418 K and different $k\%$: \diamond , 1; \triangle , 3; \bullet , 7; and \blacktriangledown , 9; (e) 423 K and different $k\%$: \diamond , 1; \square , 5; \blacktriangle , 8; and \blacksquare , 10

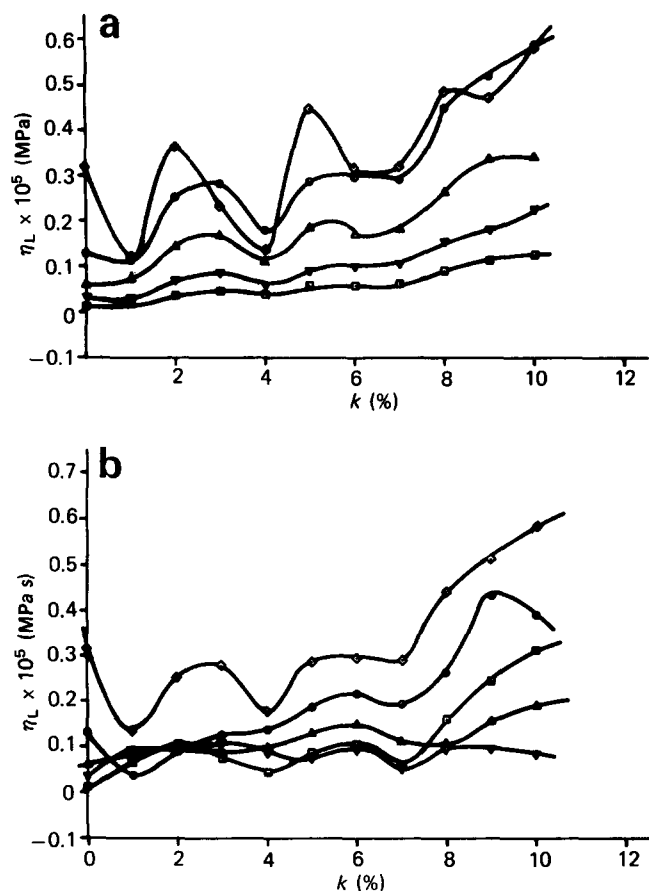


Figure 8 Longitudinal volume viscosity (η_L) as a function of volume deformation (k %) (a) at 403 K and different \dot{k} ($\times 10^{-5} \text{ s}^{-1}$): \diamond , 4.37; \circ , 10.9; \triangle , 21.8; ∇ , 43.7; \square , 109.4; (b) at $\dot{k} = 11.06 \times 10^{-5} \text{ s}^{-1}$ and different temperatures (K): \diamond , 403; \circ , 408; \triangle , 412; ∇ , 418; \square , 423

Table 2 Longitudinal volume viscosity of 1,2 s-PB at zero volume deformation (η_L^0)

\dot{k} ($\times 10^{-5} \text{ s}^{-1}$)	4.425	11.059	22.121	44.248	110.576
η_L^0 (MPa s)	0.3119	0.1248	0.0624	0.03119	0.01248

increase in segmental mobility required to contract the chains (an effect which is less noticeable as the compression rate increases, since in such circumstances the compaction of the polymer chains occurs more quickly). 1,2s-PB compressibility ($\beta = 1/V_0)(\Delta V/\Delta P)$) is shown in Figure 10 versus P (MPa) and k %. β decreases steeply until a change in slope is produced around 40–50 MPa, or $k = 3\%$. From there on β decreases more slowly as P (or k %) increases. These data compare well with those published elsewhere for other polymers¹⁸.

The displacement of the chain segments possibly provides a stiffening as well as an orientation (alignment) of the macromolecules, which enlarges the separation between them. When this phenomenon, known as dilation¹⁹, is larger than the compression phenomenon, η_L becomes negative. This effect of alignment is larger the higher the temperature, with the longitudinal volume viscosity (η_L) reaching its lowest (negative) values at $T = 412 \text{ K}$ and $\dot{k} = 20\text{--}30 \times 10^{-5} \text{ s}^{-1}$. From there on the phenomenon is reversed (less negative values of η_L the higher the temperature) due to the high degree of compaction which the chain segments have already attained. 1,2 s-PB behaves in this respect like i-PP³.

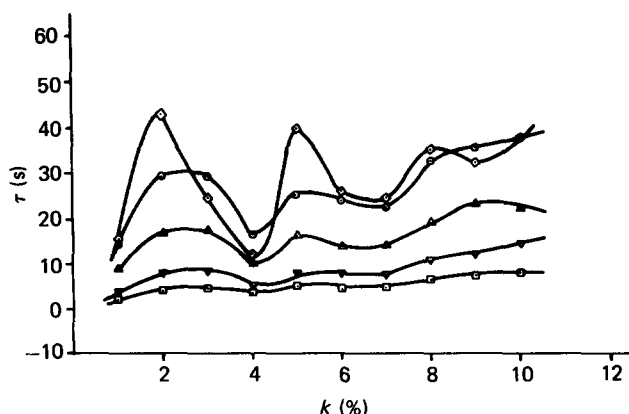


Figure 9 Retardation time (τ) as a function of volume deformation (k %) at 403 K and different \dot{k} ($\times 10^{-5} \text{ s}^{-1}$): \diamond , 4.37; \circ , 10.9; \triangle , 21.8; ∇ , 43.7; \square , 109.4

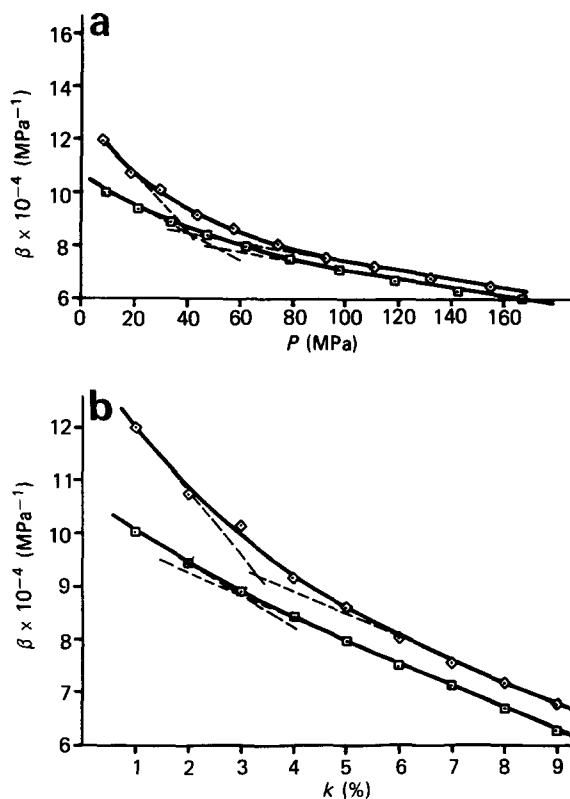


Figure 10 1,2 s-PB melt compressibility (β) at $\dot{k} \times 10^{-5} \text{ s}^{-1} = 4.37$ (\diamond) and 109.4 (\square) as a function of (a) stress (P), and (b) volume deformation (k %)

The volume reduction cannot continue forever because the volume flow comes to a halt when the resultant elastic response (rigidity or modulus of elasticity, Figure 6) due to accrued density changes builds up an internal pressure (P_i)* equal and opposed to the initial flow.

Simultaneously, this halting pressure begins to decrease by relaxation of the compressed chain segments, possibly due to changes⁸ from *trans* to *gauche*

* The internal pressure P_i is given by

$$P_i = \frac{RT}{V(T, P) - V(0)} \quad (17)$$

with $V(0)$ being the volume of the interacting unit, which may be compared to that of the structural unit².

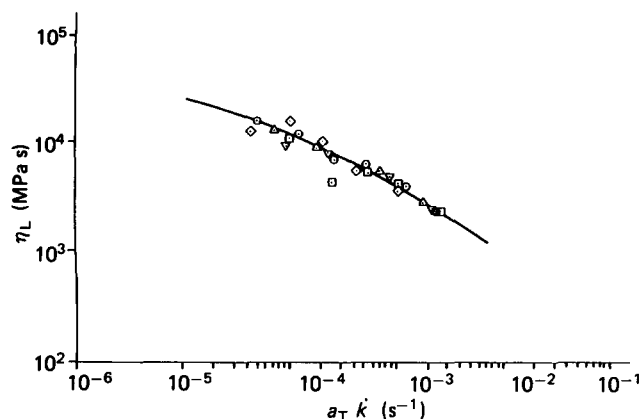


Figure 11 Longitudinal volume viscosity (η_L) as a function of temperature (K): \diamond , 403; \circ , 408; \triangle , 412; ∇ , 418; \square , 423; $k=4\%$ and $T_0=403$ K

conformation (changes in external pressure can be even more important in increasing the number of *gauche* bonds than the variation of P_i), which has a 1–6% smaller volume²⁰ than the *trans* conformation, and is a function of the bulkiness of the substituents (staggered positions where the superposition of the segments of the molecule is smaller have a greater volume).

The process of chain stiffening and relaxation is repeated again and again (Figure 8). As the volume of the macromolecule increases during internal rotation from *gauche* to *trans*, the molecule has to do work (of value $P_i \Delta V_w$, where ΔV_w is the *gauche*–*trans* molecular volume difference) to displace the surrounding continuum and to enlarge the cavity. The term $P_i \Delta V_w$ modifies the potential of internal rotation about the C–C bond and diminishes the *gauche*–*trans* energy difference ($\Delta E = \Delta H - P \Delta V_w$) because the formation of more compact structure is preferred.

The ‘waviness’ (which is a characteristic of helicoidal polymers like PMMA² and PS¹ and of flexible polymers like PEO⁴ is possibly assisted in the case of 1,2 s-PB and i-PP³ by the fact⁸ that in stereospecific polymers all of the preferred conformations of the various kinds of dyad are equivalent.

One may finally say that the compression behaviour of these macromolecules is affected by changes in external pressure, changes in internal pressure, and changes in volume (*trans*–*gauche*) of the sample.

Effect of temperature (T)

The longitudinal volume viscosity (η_L) of 1,2 s-PB at temperatures of 403–423 K, and constant volume deformation ($k\%$) is shown in Figure 7.

At the lower compression rates (\dot{k}), η_L first decreases, and then reaches a minimum at about $20 \times 10^{-5} \text{ s}^{-1}$, which is deeper at the run temperature of 412 K.

At higher compression rates (\dot{k}), η_L always decreases, approaching the limiting value $\eta_L = 0$ at $\dot{k} = \infty$.

In all cases the longitudinal volume viscosity (η_L) of 1,2 s-PB increases with increasing temperature, i.e. an increase in temperature has the same effect on ΔV as an increase in pressure, or a decrease in compression rate (\dot{k}), possibly due to the fact that the collapse of the free volume freezes out the higher energy conformations, with the corresponding increase in the number of molecular contacts, which hinder the changes in position of the atoms and molecules (intra- and inter-molecular effects

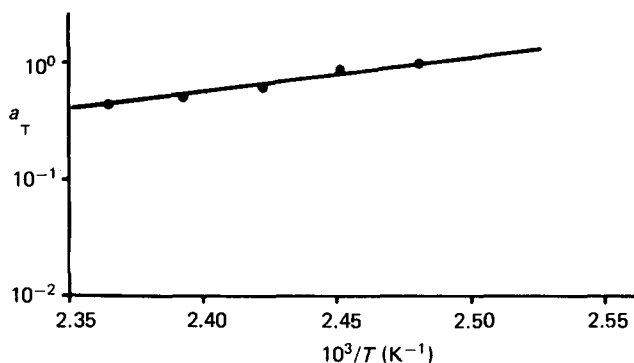


Figure 12 Effect of temperature on the shift factor a_T of 1,2 s-PB at $k=4\%$ and reference temperature $T_0=403$ K

on the molecular vibrations, which are larger the higher the experimental temperature).

The log–log plot of Figure 7 data, can be translated along the abscissa axis, and the results are shown in Figure 11 with reference temperature $T_0=403$ K. It is equivalent to multiplying the compression rate \dot{k} by a shift factor a_T . Figure 12 is a semi-logarithmic plot of these shift factors a_T versus the reciprocal temperature ($10^3/T$) for 1,2 s-PB in compression at $k=4\%$ as a representative example, and reference temperature $T_0=403$ K.

The temperature dependence of 1,2 s-PB in compression consequently obeys the Arrhenius in the form:

$$a_T = \exp \left[\frac{\Delta E}{R} \left(\frac{1}{T} - \frac{1}{T_0} \right) \right] \quad (18)$$

where R is the gas constant, and $\Delta E \approx 56.3 \text{ kJ mol}^{-1}$ at $k=4\%$ is the 1,2 s-PB temperature independent compression flow activation energy.

Combined effect of temperature and compression rate

The simultaneous effect of temperature and compression rate on the longitudinal volume viscosity is described by the plot of $\log \eta_L$ versus $\log(a_T \dot{k})$ (Figure 11). A statistical analysis of these data, using the method of least squares provides the following second-order polynomial:

$$\log \eta_L(T, \dot{k}) = A_0 + A_1 (\log a_T \dot{k}) + A_2 (\log a_T \dot{k})^2 \quad (19)$$

in which the coefficients A_0 – A_2 have the following values: $A_0=0.0603171$, $A_1=-1.72228$, $A_2=-0.18975$.

ACKNOWLEDGEMENT

Experimental measurements were made with the help of Dr C. Marco (specific heat) and Mr J. M. Fernandez-Bravo.

REFERENCES

- 1 Aleman, J. V. *Rheol. Acta* 1988, **27**, 61–68
- 2 Hurtado-Laguna, F. and Aleman, J. V. *J. Polym. Sci., Polym. Chem. Edn* 1987, in press
- 3 Alonso-Abegozar, A. and Aleman, J. V. *Makromol. Chem.* 1988, **189**, 573–585
- 4 Aleman, J. V. *J. Non-Newton. Fluid Mech.* 1987, **25**, 365–383

- 5 Sanchez-Sancha, M. and Aleman, J. V. *J. Rheol.* 1985, **29**, 307
- 6 Lesbats, J. P., Legross, R. and Aleman, J. V. *J. Polym. Sci., Polym. Chem. Edn* 1982, **20**, 1971–1984
- 7 Sanchez-Sancha, M. and Aleman, J. V. *Rheol. Acta* 1984, **23**, 31–39
- 8 Flory, P. J. 'Statistical Mechanics of Chain Molecules', Intersciences, New York, 1969
- 9 Tadokoro, H. 'Structure of Crystalline Polymers', Interscience, New York, 1979
- 10 Candia, F. and Amelino, L. *J. Macromol. Sci. Phys.* 1974, **39**, 435–445
- 11 Muruyama, T. Proc. 7th Int. Cong. Rheol. 1976, pp. 402–403
- 12 Japan Synthetic Rubber Co., JSR-RB Technical Report
- 13 Scott, R. L., Carter, W. C. and Magat, M. *J. Am. Chem. Soc.* 1949, **71**, 220–223
- 14 Dainton, F. S., Evans, D. M., Hoare, F. E. and Melia, T. P. *Polymer* 1962, **3**, 297
- 15 Conti, F., Delfini, M., Segre, A. L., Pini, D. and Porri, L. *Polymer* 1974, **15**, 816–818
- 16 Mochel, V. D. *J. Polym. Sci.* 1972, A-1, **10**, 1009–1018
- 17 Wei, K. W. and Cuculo, J. A. *J. Polym. Sci., Polym. Phys. Edn* 1980, **18**, 343–359
- 18 Ferry, J. D. 'Viscoelastic Properties of Polymers', Wiley, New York, 1980
- 19 Doi, M. and Edwards, S. F. 'Theory of Polymer Dynamics', International Series of Monographs in Physics, no. 73, Oxford Sci. Pub., 1986
- 20 Bleha, T. *Makromol. Chem. Rapid Commun.* 1981, **2**, 35–39
- 21 Schenkel, G. *Kunststofftech.* 1973, **12**, 1–7
- 22 Kovacs, A. J. *Adv. Polym. Sci.* 1964, **3**, 394